(positions 5 and 7). The N-methylation of Leu and the O-glycosylations presumably are later biosynthetic steps. With knowledge of the linear precursor peptides, the synthesis of varied linear peptides which could possibly serve as substrates for the cyclization is now being pursued in a combinatorial approach. Thus the way towards new, semi-synthetic glycopeptide antibiotics would be opened.

Experimental Section

The SP1-1-oxygenase mutant from *Amycolatopsis mediterranei* DSM5908 was fermented in a liquid culture[11] with 50 $\mu g\,mL^{-1}$ of erythromycin (output: 3.1 mg (SP-969) and 2.2 mg (SP-1134) per L of culture medium). After separation on XAD-16 adsorber resin, the peptides were purified by means of preparative HPLC (Nucleosil C18, 5 μm, 250 × 20 mm, Grom, Herrenberg, Germany), eluent: water (0.1% trifluoroacetic acid) and acetonitrile (0.1% trifluoroacetic acid).

The ES-MS and ES-MS/MS experiments were carried out with a triple quadrupole mass spectrometer (Perkin-Elmer Sciex, Thornhill, Canada) using a pneumatically supported electrospray source and argon collision gas.

The high-resolution mass spectra were recorded with the APEX-II-FT-ICR mass spectrometer 4.7T (Bruker-Franzen, Bremen, Germany) with electrospray ionization in the positive-ion mode. The calibration took place externally with PPG-1020. The resolution achieved amounts to 17000 (SP-969) and 30000 (SP-1134), respectively, with accuracies of mass of 9 and 16 ppm, respectively. The NMR experiments were carried out on a WM-400 spectrometer console (Bruker, Karlsruhe, Germany).

For the GC-MS investigation (Carlo Erba 2900/Varian MAT112S; MAT, Bremen), the peptides were hydrolyzed under a vacuum (6 N HCl, 110 °C, 24 h) and derivatized with methanol/HCl (110 °C, 15 min) and trifluoroacetic anhydride (110 °C, 10 min), respectively. Fused silica capillaries (25 m × 0.25 mm covered with L-Chirasil-Val and Lipodex E (30%), respectively, in PS255, film thickness 0.13 μm) were used as columns.

Received: December 29, 1998 [Z12848]
German version: *Angew. Chem.* **1999**, *111*, 2096–2099

Keywords: balhimycin · biosynthesis · glycopeptides · structure elucidation · vancomycin

---

[1] M. K. McCormick, W. M. Stark, G. E. Pittenger, R. C. Pittenger, G. M. McGuire, *Antibiot. Annu.* **1955–1956**, 606–611.

[2] a) G. M. Sheldrick, P. G. Jones, O. Kennard, D. H. Williams, G. A. Smith, *Nature* **1978**, *271*, 223–225; b) P. J. Loll, A. E. Bevivino, B. D. Korty, P. H. Axelson, *J. Am. Chem. Soc.* **1997**, *119*, 1516–1522; c) C. M. Harris, H. Kopecka, T. M. Harris, *J. Am. Chem. Soc.* **1983**, *105*, 6915–6922; d) S. G. Grdadolnik, P. Pristovsek, D. F. Mierke, *J. Med. Chem.* **1998**, *41*, 2090–2099.

[3] R. C. Yao, L. W. Crandall in *Glycopeptide Antibiotics* (Ed.: R. Nagarajan), Marcel Dekker, New York, **1994**, pp. 1–21.

[4] D. W. Armstrong, Y. Tang, S. Chen, Y. Zhou, C. Bagwill, J.-R. Chen, *Anal. Chem.* **1994**, *66*, 1473–1484.

[5] a) D. A. Evans, M. R. Wood, B. W. Trotter, T. I. Richardson, L. C. Barrow, J. L. Katz, *Angew. Chem.* **1998**, *110*, 2864–2868; *Angew. Chem. Int. Ed.* **1998**, *37*, 2700–2704; b) K. C. Nicolaou, S. Natarajan, H. Li, N. F. Jain, R. Hughes, M. Solomon, J. Ramanjulu, C. N. C. Boddy, M. Takayanagi, *Angew. Chem.* **1998**, *110*, 2872–2878; *Angew. Chem. Int. Ed.* **1998**, *37*, 2708–2714.

[6] A. M. A. van Wageningen, P. N. Kirkpatrick, D. H. Williams, B. R. Harris, J. K. Kershaw, N. J. Lennard, M. Jones, S. J. M. Jones, P. J. Solenberg, *Chem. Biol.* **1998**, *5*, 155–162.

[7] S. Chatterjee, E. K. S. Vijayakumar, S. R. Nadkarni, M. V. Patel, J. Blumbach, B. N. Ganguli, H.-W. Fehlhaber, H. Kogler, L. Vertesy, *J. Org. Chem.* **1994**, *59*, 3480–3484.

[8] S. Pelzer, R. Süssmuth, D. Heckmann, J. Recktenwald, P. Huber, G. Jung, W. Wohlleben, *Antimicrob. Agents Chemother.*, submitted.

[9] C. Kempter, D. Kaiser, S. Haag, G. Nicholson, V. Gnau, T. Walk, K. H. Gierling, H. Decker, H. Zähner, G. Jung, J. W. Metzger, *Angew. Chem.* **1997**, *109*, 510–513; *Angew. Chem. Int. Ed. Engl.* **1997**, *36*, 498–501.

[10] S. Braun, H.-O. Kalinowski, S. Berger, *150 and More Basic NMR Experiments*, 2nd Ed., WILEY-VCH, Weinheim, **1998**.

[11] S. Pelzer, W. Reichert, M. Huppert, D. Heckmann, W. Wohlleben, *J. Biotechnol.* **1997**, *56*, 115–128.

A Highly Luminescent Tetranuclear Silver(I) Cluster and Its Ligation-Induced Core Rearrangement**

Vincent J. Catalano,* Heidi M. Kar, and Joanna Garnas

Gold compounds, in particular gold–phosphane complexes, form inter- and intramolecular aggregates with Au–Au interactions shorter than twice the van der Waals radius.[1] Such aggregation produces numerous structural motifs that range from extended, linear chains and arrays to macromolecular clusters.[2] These assemblies often exhibit intense emissions, and the excited states are directly related to the Au···Au interaction. Recently, it was demonstrated that perturbation of this interaction forms the basis of a luminescent sensor by altering the intermolecular Au···Au separations and hence the emission properties.[3]

While the aurophilicity principle[4] has been used extensively to describe the strong, closed-shell metal–metal interactions of gold clusters, surprisingly few examples of argentophilic behavior of closely related silver analogues have been reported. In contrast, for silver compounds aggregation is not the rule, and high-nuclearity silver phosphane clusters are rarely formed.[5] The sparsity of homonuclear silver clusters may be attributed to the weaker metallophilic nature of silver compared to gold. For example, the association energy of Au···Au interactions is comparable to that of typical hydrogen bonds (ca. 5–10 $kcal\,mol^{-1}$). This energy is large enough to dictate the structure in solution and the solid state, but the weaker Ag···Ag interactions preclude such directed aggregation.

Here we report the synthesis and dynamic behavior of a tetranuclear silver cluster and its unusual core rearrangement upon further ligation. With their strong luminescence and high sensitivity to ligation, these compounds have the ability to act as solution-state sensors.

As shown in Scheme 1, reaction of two equivalents of $AgBF_4$ with 6,6-bis(diphenylphosphanyl)-2,2′-bipyridyl (P_2-bpy)[6] in trichloromethane produces a species tentatively identified as $[Ag_4(P_2\text{-bpy})_2](BF_4)_4$ on the basis of $^{31}P\{^1H\}$ NMR spectroscopy. At room temperature in $CDCl_3$, a

---

[*] Prof. V. J. Catalano, H. M. Kar, J. Garnas
Department of Chemistry
University of Nevada
Reno, NV 89557 (USA)
Fax: (+1) 775-784-6804
E-mail: vjc@unr.edu

[**] We thank the National Science Foundation (CHE-9624281) for their support of this work, and Prof. T. W. Bell for use of his fluorometer.

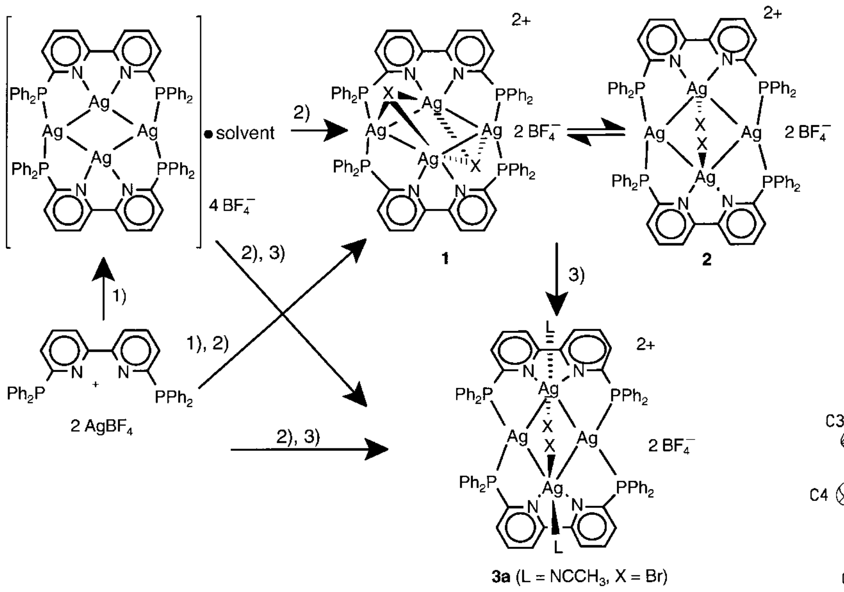

Scheme 1. Reaction of P$_2$-bpy with AgBF$_4$. 1) Solvent, 2) 2LiX, 3) CH$_3$CN or DMSO.

multiplet at $\delta = 24.7$ ($^1J(^{107}\text{Ag,P}) \approx 620$, $^1J(^{109}\text{Ag,P}) \approx 710$ Hz for the $[AM]_2[X]_4$ second-order spin system)[7] is observed. However, in CD$_3$CN a broad resonance without resolvable Ag coupling is observed at $\delta = 11.7$ and is indicative of a dynamic solvent–complex interaction. Addition of Br$^-$ or I$^-$ leads to capping of the Ag$_4$ faces and formation of the pale yellow species **1** and **2**, whereas addition of halide in the presence of a coordinating solvent produces colorless **3a** or **3b** (see below). The order of addition is inconsequential, for dissolution of an intimate mixture of solid LiBr, AgBF$_4$, and P$_2$-bpy produces the same species without loss of Ag$^+$ as AgBr. At room temperature **1** and **2** appear to interconvert on the NMR time scale.[8] In view of the solid-state structures, this dynamic behavior may be attributed to the movement of the halide ligand about the Ag$_4$ face with concurrent rearrangement of the Ag$_4$ core. Complexes **1** and **2** can be treated with a donor solvent to produce **3a** or **3b.**

Remarkably, **1** and **2** (X = Br) cocrystallize with both species present in the unit cell (Figure 1).[9] Each molecule is centrosymmetric and contains a crystallographically imposed planar Ag$_4$ core. Although the two molecules have the same composition, they exhibit significant structural differences. The main structural element of **1** is a diamondlike Ag$_4$ core, the upper and lower faces of which are capped by triply bridging bromide ions, whereas in **2** the silver ions form a nearly square core with two terminal bromide ligands. These differences are reflected in the interatomic separations, with Ag1–Ag2 and Ag1a–Ag2 distances in **1** of 3.165(2) and 2.965(2) Å, respectively, while the corresponding distances in **2** are slightly shorter (Ag3–Ag4 2.937(2), Ag3a–Ag4 2.978(2)). Although formally nonbonding, these Ag–Ag separations of about 3.0 Å may be considered as strongly interacting.[5] The shift from the diamond core in **1** to the square core in **2** is reflected in the internal angles at the silver ions. In **1** the Ag1-Ag2-Ag1a and Ag2-Ag1-Ag2a angles are 107.13(5) and 72.87(5)°, respectively. The corresponding angles in **2** (Ag3-Ag4-Ag3a 93.51(5), Ag4-Ag3-Ag4a 86.49(5)°) more closely approach the 90° of a perfectly square core. The bromide ion triply caps the Ag$_4$ core of **1** with three short Ag–Br distances (Ag1–Br1 2.768(2), Ag2–Br1 2.780(2), Ag2a–Br1 2.658(2) Å), while in **2** the bromide ions are bound to the bipyridine-coordinated Ag ions in a terminal fashion with longer distances to the neighboring Ag atoms (Ag4–Br2 2.614(2), Ag3–Br2 2.978(2), Ag3a–Br1 2.946(2) Å). A further reflection of

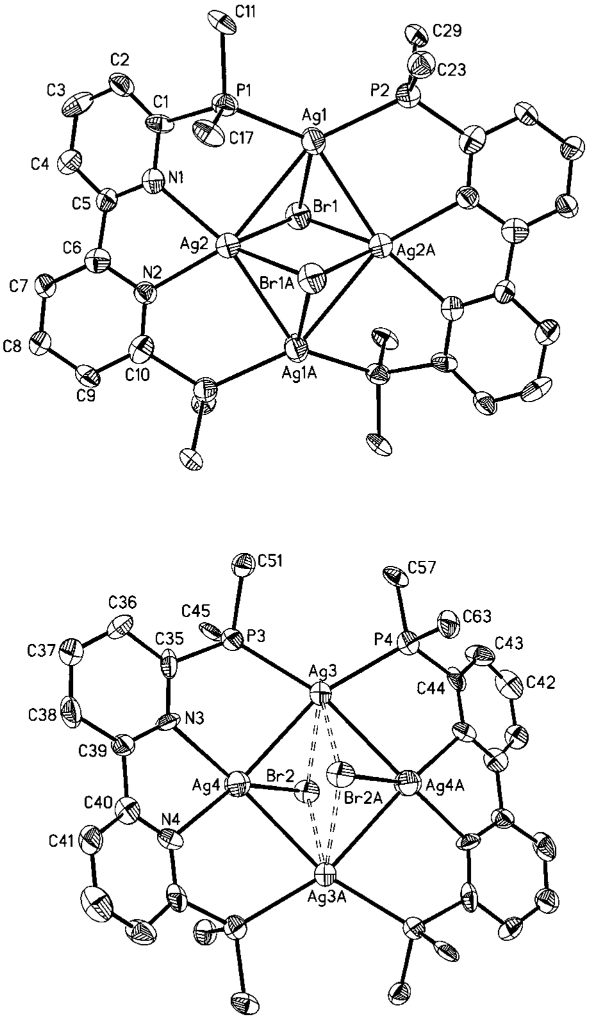

Figure 1. Thermal ellipsoid plot (50% probability) of the cores of **1** (top) and **2** (bottom) with phenyl rings and hydrogen atoms omitted for clarity. Selected bond lengths [Å] and angles [°] for **1**: Ag1–Ag2 3.165(2), Ag1–Ag2a 2.965(2), Ag1 ··· Ag1a 4.933, Ag2 ··· Ag2a 3.644, Ag1–Br1 2.768(2), Ag2–Br1 2.780(2), Ag2a–Br1 2.658(2), Ag1 ··· Br1a 3.558(2), Ag1–P1 2.468(4), Ag1–P2 2.457(4), Ag2–N1 2.301(11), Ag2–N2 2.368(11); P1-Ag1-P2 122.07(14), P2-Ag1-Ag2a 83.46(10), Ag2a-Ag1-Br1 55.11(5), Br1-Ag1-Ag2 55.39(5), Ag2-Ag1-P1 73.44(9), N1-Ag2-Ag1 88.4(3), Ag1-Ag2-Br1 55.04(5), Br1-Ag2-Br1a 95.87(6), Br1a-Ag2-Ag1a 58.68(5), Ag1a-Ag2-N2 91.4(3), N2-Ag2-N1 72.3(4), Ag1-Br1-Ag2a 66.22(5), Ag2a-Br1-Ag2a 84.13(6), Ag2-Br1-Ag1 69.57(5). Selected bond lengths [Å] and angles [°] for **2**: Ag3–Ag4 2.937(2), Ag3–Ag4a 2.978(2), Ag3 ··· Ag3a 4.309, Ag4 ··· Ag4a 4.052, Ag4–Br2 2.614(2), Ag3–Br2 2.978(2), Ag3–Br2a 2.946(2), Ag4 ··· Br2a 3.106(2), Ag3–P3 2.459(4), Ag3–P4 2.458(4), Ag4–N3 2.321(10), Ag4–N4 2.300(11); P3-Ag3-P4 118.76(13), P4-Ag3-Ag4a 76.26(10), Ag4a-Ag3-Br2a 52.36(4), Br2a-Ag3-Ag4 63.73(5), Ag4-Ag3-P3 78.57(9), N3-Ag4-Ag3 91.5(3), Ag3-Ag4-Br2 64.60(5), Br2-Ag4-Ag3a 63.20(5), Ag3a-Ag4-N4 91.7(3), N4-Ag4-N3 71.8(4), Ag4-Br2-Ag3 62.96(5), Ag3-Br2-Ag3a 93.31(5), Ag3a-Br2-Ag4 64.44(5).

these core distortions is the twisting of the bipyridine portions of the P_2-bpy ligands. In **1** the bipyridine ligand is significantly twisted with a N1-C5-C6-N2 torsion angle of 30.1°, whereas the two pyridine rings of **2** are less distorted (N3-C39-C40-N4 14.3°). All other distances are within expected ranges for similar silver phosphane[10] and bipyridine complexes.[11]

Coordination of DMSO to a mixture of **1** and **2** (X = I) quantitatively produces the centrosymmetric complex **3b** (Figure 2), which contains a rigid, diamondlike Ag_4 core with a terminal halide ligand.[12] As in **1** and **2** the crystallographic symmetry dictates a planar Ag_4 core in **3b**. The coordinated DMSO molecule binds *cis* to the halide on the bipyridine-coordinated Ag ion and thus alters the coordination geometry towards octahedral. The bipyridine ligands are bent away to accommodate the DMSO molecule, and the Ag_4 core is elongated to 4.545(2) Å along the Ag2 ··· Ag2a vector and shortened to 3.953(2) Å along the Ag1 ··· Ag1a vector. This can be compared to the diamondlike core of **1**, in which the long Ag ··· Ag axis (4.933(2) Å) lies between the phosphane-coordinated Ag ions. In spite of this marked change, the shorter Ag–Ag distances in **3b** (Ag1–Ag2 2.999(2), Ag1a–Ag2 3.024(2) Å) are quite similar to those of **1**. However, the analogous angles are different: 82.03(4) and 97.97(4)° for Ag1-Ag2-Ag1a and Ag2-Ag1-Ag2a, respectively. A similar arrangement is observed for **3a** (X = Br, L = $NCCH_3$); however, severe disorder of the counterion prevented satisfactory refinement, and its structure is not reported here.

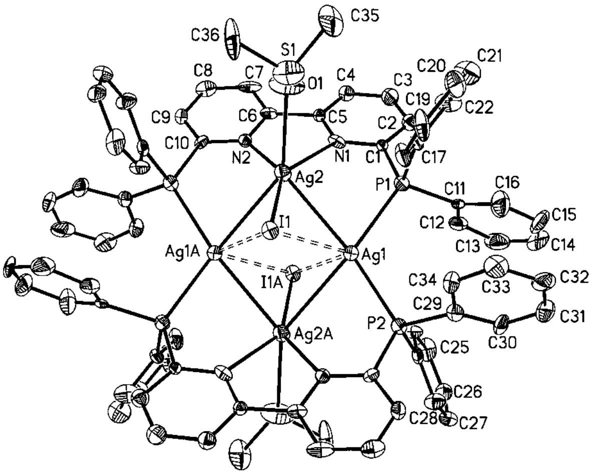

Figure 2. Thermal ellipsoid plot (50% probability) of **3b** with hydrogen atoms omitted for clarity. Selected bond lengths [Å] and angles [°]: Ag1–Ag2 2.999(2), Ag1–Ag2a 3.024(2), Ag1 ··· Ag1a 3.953, Ag2 ··· Ag2a 4.545, Ag1–I1 2.9388(14), Ag1–I1a 2.9918(15), Ag2–I1 2.7351(15), Ag2 ··· I1a 3.553(2), Ag1–P1 2.492(4), Ag1–P2 2.487(4), Ag2–N1 2.386(10), Ag2–N2 2.355(9), Ag2–O1 2.532(10); P1-Ag1-Ag2 76.23(9), Ag2-Ag1-I1 54.84(3), I1-Ag1-I1a 96.41(4), I1a-Ag1-Ag2a 54.08(3), Ag2a-Ag1-P2 75.97(9), P2-Ag1-P1 111.54(12), N2-Ag2-Ag1a 87.0(2), Ag1a-Ag2-I1 62.36(4), I1-Ag2-Ag1 61.46(4), Ag1-Ag2-N1 87.9(3), N1-Ag2-O1 78.6(3), O1-Ag2-N2 83.2(3), Ag2-I1-Ag1a 63.56(3), Ag1a-I1-Ag1 83.59(4), Ag1-I1-Ag2 63.70(4).

The Ag_4 clusters are luminescent in solution and in the solid state. Figure 3 shows the room-temperature emission of the halide-free precursor $[Ag_4(P_2\text{-bpy})_2](BF_4)_4$ in the absence of oxygen. This intense emission is sensitive to both oxygen and coordinating solvents. Exposure to air decreases the emission intensity by a factor of two, while addition of a drop of DMSO quenches the intensity by a further factor of ten. Similarly, a solution of **1** and **2** in dichloromethane shows a broad emission at 499 nm with a small shoulder at 410 nm when excited at 355 nm. Addition of acetonitrile quenches the lower energy emission but less effectively than DMSO.

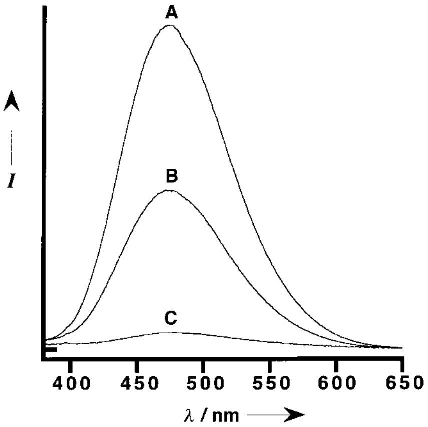

Figure 3. Emission spectra (λ_{ex} = 355 nm, 4×10^{-5} M, CH_2Cl_2) of $[Ag_4(P_2\text{-bpy})_2]^{4+}$ under N_2 (A), saturated with air (B), and with the addition of one drop of DMSO (C). I = intensity.

The photoluminescent properties of **1**–**3** can be attributed to structural rearrangements associated with ligand coordination, as are evident in the their solid-state structures. Emission between d^{10} metal centers is well known[13] and has been assigned to $d\sigma^*$–$p\sigma$ transitions for discrete d^{10} dimers,[14] to 4d–5s transitions for tetranuclear, cubane-like Ag_4 clusters,[15] to a metal-centered 5d–6s transition for the structurally similiar square-planar $[\{Au(dta)\}_4]$ (dta = dithioacetate),[16] and to a mixed-metal-centered, ligand-to-metal charge transfer (LMCT) for the closely related $[Ag_4(\mu\text{-dppm})_4(\mu_4\text{-Te})]^{2+}$ species (dppm = bis(diphenylphosphanyl)methane).[17] A MLCT transition can be ruled out because of the large Stokes shift, the lack of an accessible Ag^{II}/Ag^{I} redox couple, and the fact that the corresponding $[(AuCl)_2(P_2\text{-bpy})]$[18] complex is nonemissive. Since the halide-free material is highly luminescent, a LMCT process is unlikely. Therefore, the observed emission can be assigned to a metal-centered state analogous to that of $[\{Au(dta)\}_4]$ or of $[Ag_4(\mu\text{-dppm})_4(\mu_4\text{-Te})]^{2+}$ without the LMCT (Te $\rightarrow Ag_4$) contribution.

The ability of $[Ag_4(P_2\text{-bpy})_2]^{4+}$ to act as a sensor is demonstrated in Figure 4. The emission is significantly reduced by the presence of CO and returns to full intensity after purging with N_2. The IR spectrum of the CO adduct shows only terminal CO ligands (1993 and 2021 cm^{-1}). Interestingly, the same emission is completely quenched by addition of NO but does not return to its intial state after N_2 purging. However, evaporation of this solution in vacuo with gentle heating produces the NO-free material. A broad band at 1844 cm^{-1} (CH_2Cl_2) indicates linear NO coordination, but interference between bands at 1550 and 1650 cm^{-1} may mask stretching bands of the bent coordination mode.

As is typical of Ag^I phosphane complexes, none of the compounds reported here exhibited reversible redox behavior in cyclic voltammometry experiments. Instead, only decomposition was observed.

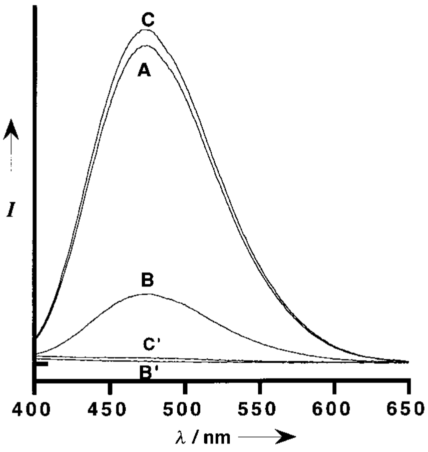

Figure 4. Emission spectra ($\lambda_{ex} = 355$ nm, CH_2Cl_2, 10^{-5} M) of $[Ag_4(P_2\text{-}bpy)_2](BF_4)_4$ under N_2 (A), saturated with CO (B), after purging with N_2 (C), saturated with NO (B′), and after purging with N_2 (C′). I = intensity.

The novelty of the Ag_4 complexes reported here resides in their unusual ligation-induced core rearrangements and the resulting photophysical properties. Unlike the numerous Au–Au compounds, the photophysical responses originate without the destruction of the metal–metal interactions. Rather, they reflect a significant rearrangement of the tetrametallic core with changing ligation. The ability to act as a solution-state sensor is demonstrated by the significant spectroscopic changes. The $[Ag_4(P_2\text{-bpy})_2]^{4+}$ species provides a useful template for exploring the metal–metal rearrangements as a function of added capping group and donor ligand. We are currently exploring these reactions and the chemical and physical properties of their products.

Experimental Section

1 and **2**: A solution of $AgBF_4$ (127.7 mg, 0.656 mmol) in methanol (20 mL) was slowly added dropwise to a solution of P_2-bpy (172.0 mg, 0.328 mmol) in dichloromethane (25 mL), and the mixture was stirred for 5 min at room temperature. A solution of LiBr (42.7 mg, 0.49 mmol) in methanol (20 mL) was then added very slowly with vigorous stirring, and the solution turned cloudy. After stirring for 10 min, the mixture was evaporated to dryness, the residue dissolved in dichloromethane, and the solution filtered through celite. Light yellow cyrstals of **1** and **2** were precipitated by addition of hexanes and collected by filtration (187.4 mg, 0.103 mmol, 63 %).

3: A solution of $AgBF_4$ (75.1 mg, 0.386 mmol) in methanol (20 mL) was slowly added dropwise to a solution of P_2-bpy (101.2 mg, 0.193 mmol) in dichloromethane (25 mL), and the mixture was stirred for 5 min at room temperature. A solution of NaI (43.4 mg, 0.290 mmol) in methanol (20 mL) was then added very slowly with vigorous stirring, and the solution eventually turned cloudy and pale yellow. After stirring for 10 min, the mixture was evaporated to dryness, the residue dissolved in dichloromethane, and the solution filtered through celite. After precipitation by addition of diethyl ether, the solid was recrystallized from DMSO/diethyl ether to afford colorless crystals of **3** (127.2 mg, 0.067 mmol, 69 %).

Received: January 14,
Revised version: March 26, 1999 [Z12910IE]
German version: *Angew. Chem.* **1999**, *111*, 2083–2086

Keywords: cluster compounds · luminescence · metal–metal interactions · sensors · silver

[1] a) C.-M. Che, W.-T. Wong, T.-F. Lai, H.-L. Kwong, *J. Chem. Soc. Chem. Commun.* **1989**, 243–244; b) C. King, J.-C. Wang, M. N. I. Khan, J. P. Fackler, Jr., *Inorg. Chem.* **1989**, *28*, 2145–2149.

[2] a) H. Schmidbaur, *Chem. Soc. Rev.* **1995**, 391–400; b) *The Chemistry of the Copper and Zinc Triads* (Eds.: A. J. Welch, S. K. Chapman), The Royal Society of Chemistry, Cambridge, **1993**, pp. 168–235.

[3] a) M. A. Mansour, W. B. Connick, R. J. Lachicotte, H. J. Gysling, R. Eisenberg, *J. Am. Chem. Soc.* **1998**, *120*, 1329–1330; b) J. C. Vickery, M. M. Olmstead, E. Y. Fung, A. L. Balch, *Angew. Chem.* **1997**, *109*, 1227–1229; *Angew. Chem. Int. Ed. Engl.* **1997**, *36*, 1179–1181.

[4] P. Pyykkö, *Chem. Rev.* **1997**, *97*, 597–636.

[5] M. Jansen, *Angew. Chem.* **1987**, *99*, 1136–1149; *Angew. Chem. Int. Ed. Engl.* **1987**, *26*, 1098–1110.

[6] R. Ziessel, *Tetraheron Lett.* **1989**, *30*, 463–466.

[7] C. W. Haigh, *J. Chem. Soc. A* **1970**, 1682.

[8] Based on $T_c \approx 0\,^{\circ}C$, a free energy of 12.5 kcal mol^{-1} is calculated for this process.

[9] a) Crystal structure determination for $\{[Ag_4Br_2(P_2\text{-bpy})_2](BF_4)_2\}_2 \cdot 4\,1{,}2\text{-}Cl_2(CH_2)_2$ (**1** and **2**): Siemens P4 diffractometer, $Mo_{K\alpha}$ radiation, $\lambda = 0.71073$ Å, $T = 298$ K, epoxy-coated crystal, crystal dimensions $0.38 \times 0.06 \times 0.38$ mm, monoclinic, space group $P2_1/c$, $a = 22.566(2)$, $b = 18.633(1)$, $c = 19.244(1)$ Å, $\beta = 110.84(1)^{\circ}$, $V = 7562.2(9)$ Å^3, $Z = 4$, $\rho_{calcd} = 1.768$ g cm^{-1}, $\mu(Mo_{K\alpha}) = 2.368$ mm^{-1}, $2\theta_{max} = 45^{\circ}$, analytical absorption correction (Xabs2), transmission factors 0.99–0.67; the structure was solved by direct methods and refined by full-matrix least-squares techniques on F_o^2. All non-hydrogen atoms were refined anisotropically, and hydrogen atoms were added to calculated positions by using a riding model with a fixed U_{ij} of 1.2 times that of the host atom. 12154 reflections, of which 9885 were unique ($R_{int} = 0.078$), 937 parameters, $R_1 = 0.0711$ ($I > 2\sigma(I)$), $wR_2 = 0.1330$, max./min. residual electron density 0.854/–0.660 e^{-1} Å^3 (maximum 0.83 Å from Br2). b) Crystallographic data (excluding structure factors) for the structures reported in this paper have been deposited with the Cambridge Crystallographic Data Center as supplementary publication no. CCDC-113399 and -113400. Copies of the data can be obtained free of charge on application to CCDC, 12 Union Road, Cambridge CB21EZ, UK (fax: (+44)1223-336-033; e-mail: deposit@ccdc.cam.ac.uk).

[10] R. E. Bachman, D. F. Andretta, *Inorg. Chem.* **1998**, *37*, 5657–5663.

[11] a) C. Kaes, M. W. Hosseini, C. E. F. Rickard, B. W. Skelton, A. H. White, *Angew. Chem.* **1998**, *110*, 970–973; *Angew. Chem. Int. Ed.* **1998**, *37*, 920–922; b) P. N. W. Baxter, J.-M. Lehn, J. Fischer, M.-T. Youinou, *Angew. Chem.* **1994**, *106*, 2432–2434; *Angew. Chem. Int. Ed. Engl.* **1994**, *33*, 2284–2287.

[12] Crystal structure determination of $[Ag_4I_2(P_2\text{-bpy})_2(dmso)_2](BF_4)_2 \cdot 4\,DMSO$, **3b**: $2\theta_{max} = 45.0^{\circ}$, $T = 193(2)$ K, crystal dimensions $0.02 \times 0.22 \times 0.02$ mm, monoclinic, space group $P2_1/c$, $a = 13.016(3)$, $b = 11.040(1)$, $c = 31.388(7)$ Å, $\beta = 97.10(1)^{\circ}$, $V = 4475.8(15)$ Å^3, $Z = 2$, $\rho_{calcd} = 1.755$ g cm^{-1}, $\mu(Mo_{K\alpha}) = 1.832$ mm^{-1}; the structure was solved by direct methods and refined by full-matrix least-squares techniques on F_o^2; 8014 reflections collected, of which 5841 were unique ($R_{int} = 0.047$), 544 parameters, $R_1 = 0.0646$ ($I > 2\sigma(I)$), $wR_2 = 0.0914$, max./min. residual electron density 0.679/–0.772 e^{-1} Å^{-3}. All non-hydrogen atoms were refined anisotropically, and hydrogen atoms were added to calculated positions by using a riding model with a fixed U_{ij} of 1.2 times that of the host atom.[9b]

[13] C. Kutal, *Coord. Chem. Rev.* **1990**, *99*, 213–252.

[14] a) J. P. Fackler, Jr., T. A. Grant, *The Chemist* **1998**, *June/July*, 29–34; b) J. M. Forward, D. Bohmann, J. P. Fackler, Jr., R. J. Staples, *Inorg. Chem.* **1995**, *34*, 6330–6336; c) C. King; J. C. Wang, M. N. I. Khan; J. P. Fackler, Jr., *Inorg. Chem.* **1989**, *28*, 2145–2149.

[15] a) P. C. Ford, A. Vogler, *Acc. Chem. Res.* **1993**, *26*, 220–226; b) M. Henary, J. I. Zink, *Inorg. Chem.* **1991**, *30*, 3111–3112; c) A. Vogler, H. Kunkely, *Chem. Phys. Lett.* **1989**, *158*, 74–76.

[16] A. Vogler, H. Kunkely, *Chem. Phys. Lett.* **1988**, *150*, 135–137.

[17] V. W.-W. Yam, K. K.-W. Lo, C.-R. Wang, K.-K. Cheung, *Inorg. Chem.* **1996**, *35*, 5116–5117.

[18] $[(AuCl)_2(P_2\text{-bpy})]$ has been structurally characterized and contains two Au–Cl moieties coordinated to the phosphane portion of the P_2-bpy ligand and no short Au···Au interactions: V. J. Catalano, H. M. Kar, unpublished results.